Using noise to determine cardiac restitution with memory

Shu Dai[1] and James P. Keener[2]
[1]*Mathematical Biosciences Institute, The Ohio State University, Columbus, Ohio 43210, USA*
[2]*Department of Mathematics, University of Utah, Salt Lake City, Utah 84112, USA*
(Received 15 December 2011; revised manuscript received 7 April 2012; published 1 June 2012)

Variation in cardiac pacing cycles, as seen, for example, in heart rate variability, has been observed for decades. Contemporarily, various mathematical models have been constructed to investigate the electrical activity of paced cardiac cells. Yet there has not been a study of these cardiac models when there is variation in the pacing cycles such as noise. We present a method that uses the stochasticity of pacing cycles to determine approximate models of the dynamics of cardiac cells, and use these models to detect bifurcations to alternans.

DOI: 10.1103/PhysRevE.85.061902 PACS number(s): 87.19.Hh, 87.18.Tt

I. INTRODUCTION

The mathematical study of the dynamics of the electrical activity of cardiac cells has a long history. One of the primary problems is to determine the response of a cardiac cell to periodic stimuli and to identify and characterize bifurcations in these behaviors. While detailed ionic models have been used extensively for this study [1–6], mapping models, pioneered by Nolasco *et al*. [7,8], have been introduced in past decades to focus on the *restitution*, i.e., the dependence of and action potential durations (APDs) on the preceding diastolic interval (DI). In particular, period-doubling bifurcation occurs as the exterior stimuli pace sufficiently fast and alternation of APDs, which is called *alternans*, emerges, as illustrated in Fig. 1. Recent mapping models involve memory variables in the restitution, which are often related to the intracellular ion (mostly calcium) concentrations in different compartments, to explain more complicated restitutions [9–16]. The memories in those models are usually hidden and difficult to detect in experiments; hence, it is difficult to reconstruct the model directly. The method we develop in this paper provides one way to approximate the restitution by an alternative form, using stochastic pacing cycles, and we assume only pacing cycles and APDs are detectable.

The simple mapping model proposed in [7] suggests that the preceding DI completely determined the APD; i.e.,

$$A_n = f(D_{n-1}) \tag{1.1}$$

for some restitution function f, where A_n and D_n represent the nth APD and DI, respectively. With a fixed basic cycle length (BCL) with $A_n + D_n = \mathrm{BCL} \equiv \mu$, (1.1) becomes a simple one-dimensional (1D) map. Typically, f is a nondecreasing function of D, so there is a unique fixed point A^* which is an increasing function of μ. This is referred to as a 1:1 response. A period-doubling bifurcation (2:2 response) occurs if $f'(D^*)$ increases across 1 as μ decreases, where $D^* = \mu - A^*$, and alternans emerges as a long-short alternation of APD.

Memories are introduced recently for more complicated dynamics that are not explained by the simple 1D maps. We can summarize the general form of a model involving J memory variables as

$$\begin{aligned} A_n &= f\left(D_{n-1}, M_n^{(1)}, M_n^{(2)}, \ldots, M_n^{(J)}\right), \\ M_n^{(i)} &= g_i\left(A_{n-1}, M_{n-1}^{(i)}, T_{n-1}\right), \quad \text{for } i = 1,2,\ldots,J, \\ D_n &= T_n - A_n, \end{aligned} \tag{1.2}$$

where A_n is the nth APD, T_n is the time between the nth and $(n+1)$th exterior stimuli, D_n is the DI following A_n, and $M_n^{(i)}$ are the memory variables at the time that the nth stimulus occurs. Figure 2 illustrates the variables in the model, with one memory variable shown.

A given series of stimulus intervals $\{T_n\}$ is called a pacing cycle protocol. For typical memory models, when T_n's are constant μ (S1 protocol), the system (1.2) has a fixed point $(A^*, M_*^{(1)}, M_*^{(2)}, \ldots, M_*^{(J)})$ if μ is sufficiently large. The fixed point may lose its stability through a period-doubling bifurcation to alternans when μ is below some critical value μ_c. The solid and dashed curves in Fig. 1 illustrate a typical bifurcation diagram (only values of APDs are shown in the graph).

In many situations, the pacing intervals T_n are nonconstant; i.e., there is variation in the times between consecutive stimuli. For example, in real hearts, heart rate variability is well known [17–19]. Figure 3 shows an example of a series of natural pacing cycles for a healthy human heart [20].

When the pacing intervals T_n are nonconstant, in the long time run, we do not expect convergence to a fixed point or alternans. However, if the variation in T_n's is small enough, it may be that in the long run the APDs are located in a neighborhood of the fixed point or alternans, such as the shaded region shown in Fig. 1. Thus, even in the presence of noise, there is some information about bifurcations to be gleaned from the APDs, but how much is not yet known.

In this paper we discuss the following question: Given a (random) sequence of pacing times T_n and the corresponding APDs A_n, to what extent can the restitution function f and the resulting bifurcation structure and dynamics be

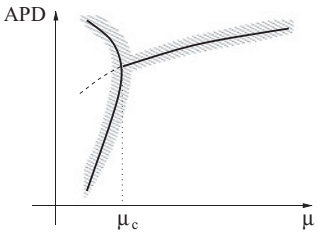

FIG. 1. Typical bifurcation diagram for a cardiac mapping model with constant cycle length μ, where period-doubling bifurcation occurs at $\mu = \mu_c$. The shaded region indicates the range of APDs when the cycle length has a small random fluctuation around μ.

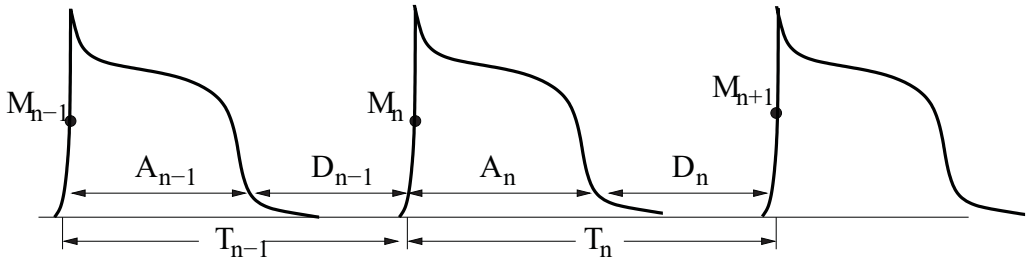

FIG. 2. Illustration of the cycle lengths T_n, action potential duration A_n, diastolic interval D_n, and memory variable M_n.

determined? To make initial progress, we assume that the data are generated by some mapping model of the form (1.2). Thus, we are provided with a series of T_n's and corresponding A_n's; however, the memory terms $M_n^{(i)}$ in (1.2) are hidden variables and cannot be detected. In what follows we develop a regression algorithm with which we are able to obtain an approximate equivalent form having dynamics similar to (1.2). Furthermore, since the data are generated by a known model, we have a check for how good our approximate restitution function and bifurcation structure are.

The organization of the paper is as follows. In Sec. II we introduce our ideas using a simple memory model proposed by Tolkacheva *et al.* [21]. In Sec. III, we discuss a more general mapping model with one memory variable, using a model suggested by Fox *et al.* [22] as an example. In Sec. IV we discuss the most general case of a mapping model with multiple memory variables, as in (1.2). Section V is the discussion, and Sec. VI is the conclusion.

II. APPROXIMATE TOLKACHEVA *ET AL.* MODEL

The mapping model proposed by Tolkacheva *et al.* [21] is in the form

$$A_n = f(D_{n-1}, A_{n-1}), \tag{2.1}$$

which is a special case of the general mapping model (1.2) with $J = 1$ and $M_n^{(1)} = A_{n-1}$. The details of the model are given in the Appendix. If A^* is a fixed point when the pacing intervals are the constant μ, its stability is determined by the derivative

$$f' = \left.\frac{df}{dA}\right|_{A^*} = -\left.\frac{\partial f}{\partial D}\right|_{D^*} + \left.\frac{\partial f}{\partial A}\right|_{A^*},$$

where $D^* = \mu - A^*$.

Previous analysis has shown that in the 1:1 response case, one can estimate f' from experiments by the following process (for more details see [21]). First, for a given BCL μ, the fixed

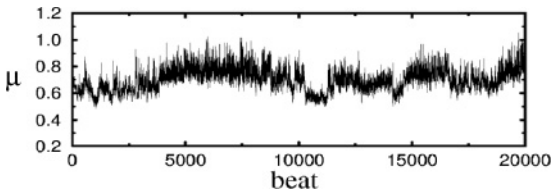

FIG. 3. Sequence of interbeat intervals (in seconds) for a healthy individual [20].

point A^* and associated D^* satisfy

$$A^* = f(D^*, A^*) = f(\mu - A^*, A^*),$$

and we record the fixed points A^* and associated D^* for different BCLs to obtain the *dynamic restitution curve* (RC). The slope of the dynamic RC at a particular (A^*, D^*) that we are interested in is estimated by

$$S_{\text{dyn}} = \frac{\partial A^*}{\partial D^*} = \frac{\partial f/\partial D_{n-1}|_{A_{n-1}=A*}}{1 - \partial f/\partial D_{n-1}|_{A_{n-1}=A*}}.$$

Then, we use the S1-S2 stimulus protocol: a long series of constant stimulus intervals, $\mu_{S1} = \mu$, followed by a single stimulus with a different interval μ_{S2}. The measured APD A_{S1S2} is given by

$$A_{S1S2} = f(D_{S1S2}, A^*),$$

where A^* is the fixed point corresponding to BCL $\mu_{S1} = \mu$ and $D_{S1S2} = \mu_{S2} - A^*$, and the S1-S2 RC is the plot of A_{S1S2} versus D_{S1S2}. The slope of the S1-S2 RC at $D_* = \mu - A^*$ is given by

$$S_{S1S2} = \left.\frac{dA_{S1S2}}{dD_{S1S2}}\right|_{D_{S1S2}=D^*} = \left.\frac{\partial f}{\partial D_{n-1}}\right|_{A_{n-1}=A^*}. \tag{2.2}$$

The two slopes S_{dyn} and S_{S1S2} can be estimated by the finite difference method in experiments, and the value of f' follows from the chain rule:

$$f' = 1 - \left(1 + \frac{1}{S_{\text{dyn}}}\right) S_{S1S2}. \tag{2.3}$$

The method we implement below to approximate f is to make the pacing cycles stochastic, which we call the "stochastic protocol." We show that we can approximate the dynamics of the mapping model (2.1) in an interval $[\mu_a, \mu_b]$ rather than simply at a single point as in (2.3). Furthermore, we can include cases when a period 2 bifurcation occurs and alternans appears in the interval $[\mu_a, \mu_b]$.

We assume the pacing cycles T_n are randomly distributed in $[\mu_a, \mu_b]$, and the action potential durations A_n are generated through (A1) with a random initial value. We define $\bar{T}$ to be the sample mean of the cycles T_n; i.e.,

$$\bar{T} = \text{mean}(T_n). \tag{2.4}$$

If the variation of the cycles, i.e., the range of the interval $\mu_b - \mu_a$, is small, we may regard all T_n's as perturbations of μ. For simplicity, we first consider the 1:1 response case. In the case of constant pacing with cycle μ, there is a stable fixed

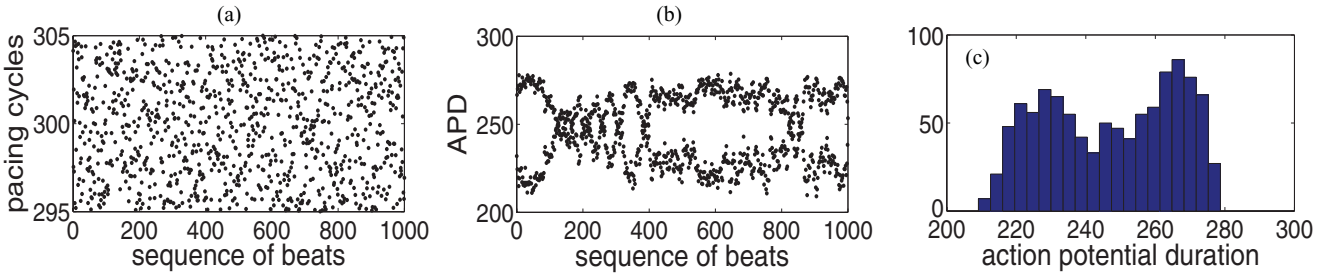

FIG. 4. (Color online) (a) Sequence of pacing cycles, (b) sequence of corresponding APDs, and (c) histogram of all APDs.

point A^*, such that

$$A^* = f(D^*, A^*), \tag{2.5}$$

where $D^* = \mu - A^*$. Since T_n's are perturbations of μ, we naturally assume all A_n's are small perturbations around A^*. The leading order approximation is

$$a_n \sim f_1 d_{n-1} + f_2 a_{n-1} = \widetilde{f}_1 a_{n-1} + \widetilde{f}_2 t_{n-1}, \tag{2.6}$$

where $a_n = A_n - A^*$, $d_n = D_n - D^*$, and f_1 and f_2 are the partial derivatives of f with respect to D_{n-1} and A_{n-1} at the fixed point, and $\widetilde{f}_1 = f_2 - f_1$, $\widetilde{f}_2 = f_1$. We take the covariance of Eq. (2.6) with a_n and t_n, respectively, to obtain two approximating equations,

$$\begin{aligned} \langle a_n, t_{n-1}\rangle &\sim \widetilde{f}_1 \langle a_{n-1}, t_{n-1}\rangle + \widetilde{f}_2 \langle t_{n-1}, t_{n-1}\rangle, \\ \langle a_n, a_{n-1}\rangle &\sim \widetilde{f}_1 \langle a_{n-1}, a_{n-1}\rangle + \widetilde{f}_2 \langle t_{n-1}, a_{n-1}\rangle. \end{aligned} \tag{2.7}$$

Then the derivatives $\widetilde{f}_1$ and $\widetilde{f}_2$ may be determined directly by solving the above two-dimensional linear system.

The above process is equivalent to using simple linear regression to find the best least squares fit of Eqs. (2.6) with two unknown coefficients. The method of fitting data in a least squares sense has been applied widely in previous research [13,23], in which some functional form of the restitution is proposed and unknown parameters are then determined by regression analysis, i.e., by minimizing the squared error of the fit.

Here we do not assume a particular form for the restitution function f; i.e., f is completely unknown. We extend the above case of a linear approximation (2.6) to higher orders, i.e., by considering the Taylor polynomial expansion of f. In general, we are looking for a polynomial $H_1^p(A_{n-1}, T_{n-1})$ of given order p in the following form:

$$\begin{aligned} A_n &\sim H_1^p(A_{n-1}, T_{n-1}) \\ &= \sum_{0 \leqslant \alpha+\beta \leqslant p} f_{\alpha\beta} (A_{n-1} - \bar{A})^\alpha (T_{n-1} - \bar{T})^\beta, \end{aligned} \tag{2.8}$$

which best fits the given data of T_n and A_n. Here $\bar{T}$ and $\bar{A}$ are the means of the pacing cycles T_n and APDs A_n, respectively. The subscript 1 in H_1^p indicates that the restitution function $f(D_{n-1}, A_{n-1})$ depends only on the most recent previous beat. The unknown coefficients $f_{\alpha\beta}$ are to be determined. We note that $\bar{A}$ is not the fixed point solution A^* corresponding to $\bar{T}$; however, we can compute A^* from (2.8) once the coefficients are found.

To carry out this procedure for a specific example, we pick $N = 1000$ pseudorandom pacing cycles T_n, which are uniformly distributed[1] in the time interval $[\mu_a, \mu_b]$ with $\mu_a = 295$ ms and $\mu_b = 305$ ms. The theoretical bifurcation point $\mu_c \approx 301.40$ ms is located in this interval. We record the series of corresponding APDs A_n generated through the original model (A1). To mimic the measurement error of APDs in experiments, we add small noise to A_n, after the sequence is generated,

$$A_n \to A_n + \epsilon \xi_n, \tag{2.9}$$

where $\epsilon = 0.01$ ms is the magnitude of error, and ξ_n's are independent and identically distributed standard normal random variables. For convenience, we do not change the notation for A_n. We assume the error in measuring pacing cycles is negligible. The sequences of T_n and A_n are shown in Fig. 4. We also plot a histogram of the APDs in Fig. 4, from which we observe an apparent distribution involving alternans.

To obtain a period-doubling bifurcation from the approximating polynomial H_1^p, it is required that $p \geqslant 2$. We use linear regression to find the coefficients $f_{\alpha\beta}$ for each p of interest. Table I shows a statistical analysis for the case $p = 2$, for which there are six unknown coefficients $f_{\alpha\beta}$.

We repeat the above process for various values of order p using the same data set. After obtaining the coefficients $f_{\alpha\beta}$, we compare the approximate iterative function $H_1^p(A_{n-1}, T_{n-1})$ with the original model. In Fig. 5 we show their bifurcation diagrams for $p = 2,4,5$, respectively. One can observe that

[1]Uniform distribution is used as an example. In fact our approach does not depend on the distribution type of the pacing cycles. See the discussion in Sec. V.

TABLE I. Statistical analysis for regression method for approximating iteration map H_1^p for $p = 2$. There are 1000 data points, 6 unknown coefficients $f_{\alpha\beta}$, and 994 degrees of freedom. The residual standard error is 0.04221. Robustness is ensured by the following statistical criteria: multiple R squared is 1, adjusted R squared is 1, the F-statistic value is 4.04×10^7 on 5 and 994 degrees of freedom, and the p value is below 2.2×10^{-16}.

Coefficients	Estimate	Standard error	t value	Pr(>|t|)
$f_{0,0}$	249.6	2.624×10^{-3}	95096.64	$<2 \times 10^{-16}$
$f_{1,0}$	−0.9889	7.132×10^{-5}	−13865.51	$<2 \times 10^{-16}$
$f_{0,1}$	1.074	4.593×10^{-4}	2338.70	$<2 \times 10^{-16}$
$f_{2,0}$	-6.566×10^{-3}	4.676×10^{-6}	−1404.23	$<2 \times 10^{-16}$
$f_{1,1}$	1.148×10^{-2}	2.410×10^{-5}	476.27	$<2 \times 10^{-16}$
$f_{0,2}$	-5.947×10^{-3}	1.814×10^{-4}	−32.79	$<2 \times 10^{-16}$

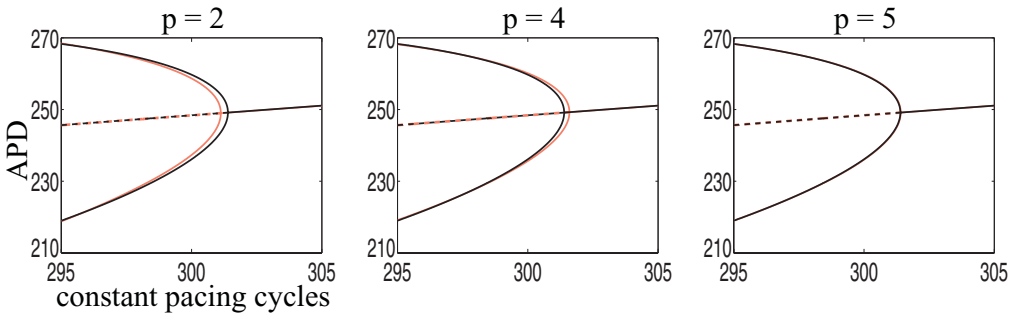

FIG. 5. (Color online) Comparison of the bifurcation diagrams between the theoretical map (A1) (black) and the approximate form (2.8) (red, light grey) for various orders of p. The solid curve indicates stability and the dashed curve indicates instability. Note that for all cases the approximate fixed points are very close to the theory and they are not distinguishable in the graph. In addition, for the case $p = 5$, the theoretical and approximate diagrams almost coincide.

with order $p = 5$, the dynamics of H_1^p is very close to the theoretical prediction.

It is obvious that for larger order p, the approximation becomes more accurate. However, there are also more undetermined coefficients $f_{\alpha\beta}$ in (2.8). Let $\ell = \ell(k,p)$ be the number of the undetermined coefficients $f_{\alpha\beta}$ in H_k^p in (2.8), where $k = 1$ indicates dependence on only the most recent stimulus interval T_{n-1}.

Two statistical values are significant to judge the accuracy of the approximation: the residual sum of squares (RSS),

$$R_{ss} = \sum \left[A_n - H_1^p(D_{n-1}, A_{n-1})\right]^2, \tag{2.10}$$

and the residual standard error (RSE),

$$r_{se} = \sqrt{\frac{R_{ss}}{N-\ell}}. \tag{2.11}$$

As we increase the order of the approximate function H_1^p, the RSS and RSE both decrease, but ℓ increases. Table II shows the values of ℓ, RSS, and RSE for different orders p. Notice that as p increases from 2 to 5, there is a significant decrease in both RSS and RSE; however, there is very little improvement as p is increased further, even though the number of parameters increases substantially. Therefore, it appears that $p = 5$ is in some heuristic sense "optimal." In the next section, we provide a less heuristic criterion to determine the "best" fit.

TABLE II. Values of ℓ, residual sum of squares (RSS), and residual standard error (RSE) for the approximate function H_1^p of different order p for Tolkacheva *et al.*'s model.

p	ℓ	RSS	RSE
2	6	1.771	0.04221
3	10	1.639	0.04069
4	15	0.2382	0.01555
5	21	0.1986	0.01424
6	28	0.1975	0.01425
7	36	0.1963	0.01427

III. APPROXIMATE FOX *ET AL.* MODEL: AN EXAMPLE OF A MAPPING MODEL WITH ONE MEMORY VARIABLE

The mapping model with one memory variable in the form

$$\begin{aligned} A_n &= f(D_{n-1}, M_n), \\ M_n &= g(A_{n-1}, M_{n-1}, T_{n-1}), \\ D_n &= T_n - A_n, \end{aligned} \tag{3.1}$$

is regarded as a good approximation for the behavior of quite a few ionic models [9,22,24,25]. A specific example of (3.1) is the model by Fox *et al.* [22], which is described in detail in (A5).

We start with the model (3.1). Some expanded forms of (3.1) were considered by previous researchers. For instance, in [26] the authors proposed that

$$A_n = f(D_{n-1}, A_{n-1}, D_{n-2}, A_{n-2}, \ldots)$$

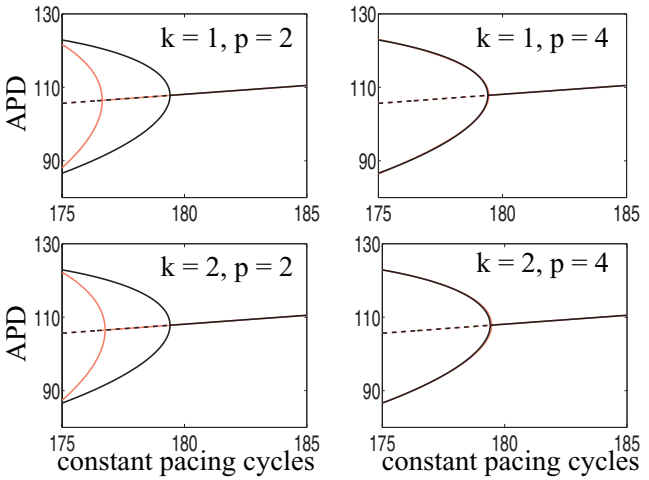

FIG. 6. (Color online) Comparison of the bifurcation diagrams between the theoretical map (3.1) (black) and the approximate form (3.5) (red, light grey) for various values of k and p. The solid line indicates stability and the dashed line indicates instability. We note that in each of the two cases, $(k,p) = (1,4)$ and $(2,4)$, the dynamics of theory and the approximation are very close and their bifurcation diagrams almost coincide.

TABLE III. RSS, RSE, and BIC values of the approximate function H_k^p for Fox *et al.*'s model for some significant cases of (k,p) pairs, where $k \geqslant 0$, $p \geqslant 2$, and $\ell(k,p) < N/2$. The bold values correspond to the optimal selection which has the minimal BIC value.

k	p	$\ell(k,p)$	RSS	RSE	BIC	k	p	$\ell(k,p)$	RSS	RSE	BIC
0	2	3	11.36	0.1067	−4457	3	2	15	8.317	0.09189	−4686
0	3	4	3.51	0.05936	−5625	3	3	35	1.426	0.03844	−6311
0	4	5	1.941	0.04417	−6210	3	4	70	0.1829	0.01402	−8123
0	5	6	1.937	0.04415	−6205	3	5	126	0.1631	0.01366	−7851
⋮	⋮	⋮	⋮	⋮	⋮	3	6	210	0.151	0.01383	−7348
1	2	6	8.615	0.0931	−4713	⋮	⋮	⋮	⋮	⋮	⋮
1	3	10	1.635	0.04064	−6347	4	2	21	8.176	0.09139	−4662
1	4	15	0.242	0.01568	−8223	4	3	56	1.342	0.0377	−6227
1	5	21	0.2247	0.01515	−8256	4	4	126	0.1734	0.01409	−7790
1	6	28	0.2225	0.01513	−8217	4	5	252	0.1453	0.01394	−7096
⋮	⋮	⋮	⋮	⋮	⋮	⋮	⋮	⋮	⋮	⋮	⋮
2	2	10	8.491	0.09261	−4700	5	2	28	7.887	0.09008	−4649
2	3	20	1.523	0.03942	−6349	5	3	84	1.278	0.03735	−6082
2	**4**	**35**	**0.1906**	**0.01405**	**−8323**	5	4	210	0.1587	0.01418	−7298
2	5	56	0.1734	0.01355	−8273	5	5	462	0.1077	0.01415	−5945
2	6	84	0.1678	0.01354	−8112	⋮	⋮	⋮	⋮	⋮	⋮
⋮	⋮	⋮	⋮	⋮	⋮	10	2	78	7.058	0.08749	−4415
						10	3	364	0.8494	0.03655	−4557

and analyzed the different restitution curves in the restitution portrait [27]. However, to best apply our method, we need a different form which is more "compact." If we substitute the memory terms M_k of the second equation into the first equation in (3.1) for $k = n, n-1, \ldots$, we may write

$$A_n = F_n(A_0, M_0; A_{n-1}, A_{n-2}, \ldots, A_1; T_{n-1}, T_{n-2}, \ldots, T_0), \tag{3.2}$$

using that $D_n = T_n - A_n$. The function F_n in (3.2) is some combination of compositions of f and g, and A_0 and M_0 are initial values. We note that the functions F_n are different for each n. We call (3.2) the expansion form of the mapping model (3.1). If we substitute Eq. (3.2) for A_{n-2}, A_{n-3}, ... into the equation for A_n, we may rewrite (3.2) as

$$A_n = \widetilde{F}_n(A_0, M_0, A_{n-1}; T_{n-1}, T_{n-2}, \ldots, T_0), \tag{3.3}$$

for some function $\widetilde{F}_n$, which also depends on n.

In the long time run, one would expect that the information of the distant past should have little impact on the current APD, which suggests that we make the following approximation: for sufficiently large n, there are iterative maps H_k in the following form, for $k = 1,2, \ldots$:

$$A_n \sim H_k(A_{n-1}; T_{n-1}, T_{n-2}, \ldots, T_{n-k}), \tag{3.4}$$

which approximates the dynamics of (1.2); i.e., the function H_k is some approximation which only includes the most recent k memories. That this approximation is valid remains a conjecture, although a rigorous proof can be given for some particular models, for example, the model proposed by Schaeffer *et al.* [25], in which the memory M_n only depends on A_{n-1} and T_{n-1}. It is obvious that for larger k, the approximation cannot be less accurate.

The analytical form of the function H_k is unknown in general; however, H_k may be approximated by some polynomial $H_k^p(A_{n-1}; T_{n-1}, T_{n-2}, \ldots, T_{n-k})$ for $k \geqslant 0$ and $p \geqslant 2$ in the

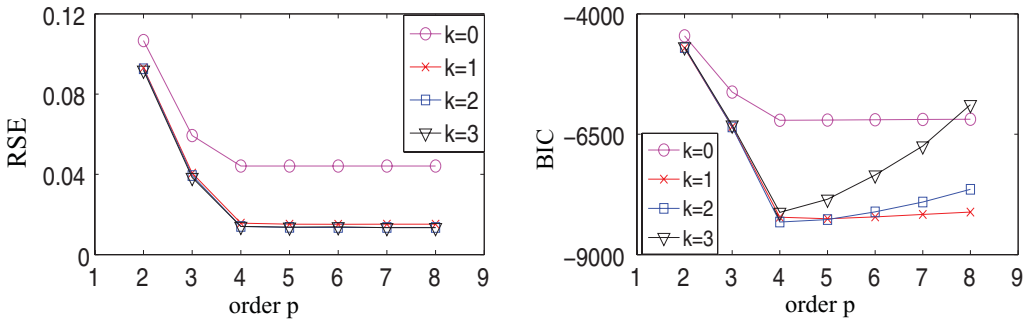

FIG. 7. (Color online) Approximate the model of Fox *et al.*: RSE and BIC values of each polynomial H_k^p vs p for $k = 0,1,2,3$.

TABLE IV. RSS, RSE and BIC values of the approximate function H_k^p for Tolkacheva *et al.*'s model for some significant cases of (k,p) pairs. The best choice of (k,p) is (1,5). The best choice of (k,p) is (1,5), which has the minimal BIC value, as shown bold in the table.

k	p	$\ell(k,p)$	RSS	RSE	BIC
0	3	4	65.78	0.257	−2694
0	4	5	63.34	0.2523	−2725
⋮	⋮	⋮	⋮	⋮	
1	3	10	1.639	0.04069	−6344
1	4	15	0.2382	0.01555	−8239
1	**5**	**21**	**0.1986**	**0.01424**	**−8379**
1	6	28	0.1975	0.01425	−8337
⋮	⋮	⋮	⋮	⋮	
2	4	35	0.2284	0.01538	−8143
2	5	56	0.1889	0.01415	−8188
2	6	84	0.1857	0.01424	−8011

following form:

$$A_n \sim H_k^p(A_{n-1};T_{n-1},T_{n-2},\ldots,T_{n-k}) = \sum h_{\alpha\beta_1\beta_2\cdots\beta_k}(A_{n-1}-\bar{A})^{\alpha}(T_{n-1}-\bar{T})^{\beta_1} \times (T_{n-2}-\bar{T})^{\beta_2}\cdots(T_{n-k}-\bar{T})^{\beta_k}, \quad (3.5)$$

where k denotes that the approximation involves information from previous k beats, p is the order of the approximate polynomial, and the summation is taken over the nonnegative indices $\alpha+\beta_1+\cdots+\beta_k \leqslant p$.

Now to approximate H_k^p we assume that the pacing cycles T_n are random and, with some random initial value, we generate $N=1000$ data points for the sequence of A_n's using Fox *et al.*'s model (A5). We also add a noise term $\epsilon\xi_n$ to each A_n as in (2.9) to mimic the error in measuring APDs, with $\epsilon=0.01$ ms. Then, given a set of data groups $(A_n,A_{n-1},T_{n-1},\ldots,T_{n-k})$, we use the regression method to estimate the best choice of the unknown coefficients $h_{\alpha\beta_1\beta_2\cdots\beta_k}$ to obtain the approximate form (3.5). We then compare the bifurcation diagrams of the original Fox *et al.* model (A5) and of the approximate form (3.5), shown in Fig. 6 for several values of k and p.

Notice that for larger k and p, the approximation is increasingly accurate (as expected). However, the total number of unknown coefficients, $\ell(k,p)$, also becomes larger. Therefore, the "optimal" parameter choice should in some way minimize the error as well as the number of unknown coefficients. One useful way to determine the best parameter set is to minimize the Bayesian information criterion (BIC) function [28],

$$B(k,p) = N\ln\left(\frac{R_{ss}}{N}\right) + \ell(k,p)\ln(N), \quad (3.6)$$

where R_{ss} is the RSS defined in (2.10).

In Table III we show RSS, RSE, and BIC values for several cases of (k,p), and Fig. 7 shows the RSE and BIC versus p for different values of k. Once again, we see that the RSE decreases rapidly until $p=4$, but there is very little improvement for larger values of p. Also, the BIC decreases as p increases to 4, but then increases for larger values of p due to the fact that

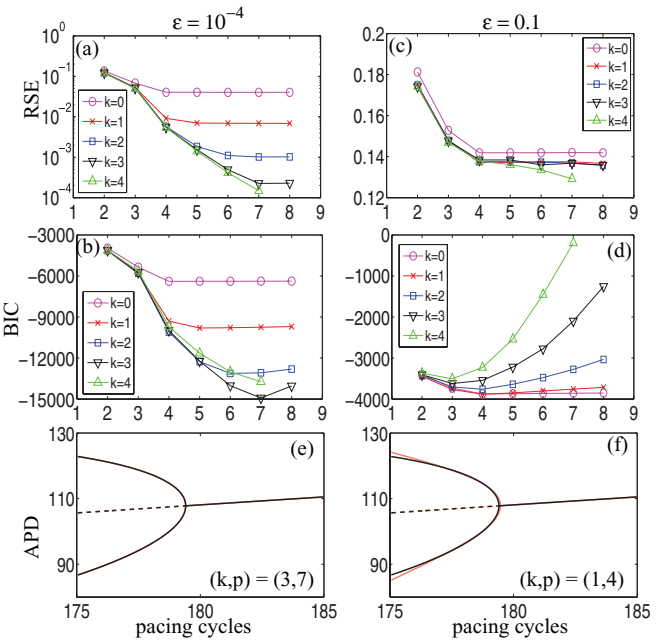

FIG. 9. (Color online) The RSE and BIC values of the approximate polynomial H_k^p vs the order p for various k, and bifurcation diagrams of H_k^p at optimal choice of (k,p) for different measurement error $\epsilon=10^{-4}$ (a, c, e) and $\epsilon=0.1$ (b, d, f), respectively, for Fox *et al.*'s model. In (e) and (f), the theoretical bifurcation diagram (black) and the approximation (red, light grey) are drawn for comparison, and in (e) the theory and approximation almost coincide.

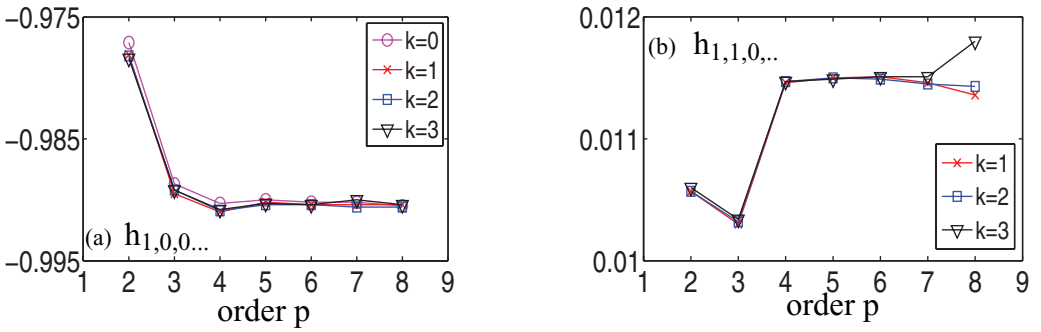

FIG. 8. (Color online) (a) The value of $h_{1,0,0,\ldots}$, the coefficient for $(A_{n-1}-\bar{A})$ vs the order p for different values of k, and (b) the value of $h_{1,1,0,\ldots}$, the coefficient for $(A_{n-1}-\bar{A})(T_{n-1}-\bar{T})$ vs the order p for different values of k.

TABLE V. Optimal choice of (k,p) and corresponding RSE vs different number of data points N and measurement error ϵ. We are able to detect earlier memory and achieve better accuracy if we have more data points or lower measurement error.

	$\epsilon = 10^{-4}$		$\epsilon = 0.01$		$\epsilon = 0.1$	
N	optimal (k,p)	RSE	optimal (k,p)	RSE	optimal (k,p)	RSE
30	(1,4)	0.005963	(1,3)	0.01691	(0,2)	0.1299
100	(1,5)	0.006378	(1,4)	0.01644	(0,3)	0.1389
300	(3,5)	0.000235	(1,5)	0.01642	(0,4)	0.1385
1000	(3,7)	0.000225	(2,4)	0.01405	(1,4)	0.1372
3000	(3,7)	0.000228	(2,5)	0.01419	(1,4)	0.1414

RSE is decreasing slowly while $\ell(k,p)$ is increasing rapidly as a function of p. Since the BIC is minimized at $k=2$ and $p=4$, we take the polynomial $H_{2,4}(A_{n-1};T_{n-1},T_{n-2})$, i.e.,

$$\begin{aligned} A_n &\sim H_{2,4}(A_{n-1};T_{n-1},T_{n-2}) \\ &= \sum_{0\leqslant\alpha+\beta_1+\beta_2\leqslant 4} h_{\alpha\beta_1\beta_2}(A_{n-1}-\bar{A})^{\alpha} \\ &\quad \times (T_{n-1}-\bar{T})^{\beta_1}(T_{n-2}-\bar{T})^{\beta_2}, \end{aligned} \tag{3.7}$$

where the coefficients $h_{\alpha\beta_1\beta_2}$ are determined by the regression method to be the "best" approximation of Fox *et al.*'s model.

Now we come back to the model by Tolkacheva *et al.* discussed in Sec. II. We assume that the model is in the general form (3.1), and we repeat the previous process for different values of (k,p). We show the results for some significant cases of (k,p) in Table IV. Notice that the choice of (k,p) that minimizes the BIC is (1,5).

IV. GENERAL MAPPING MODEL WITH MULTIPLE MEMORY VARIABLES

For the most general mapping model with multiple memory variables (1.2), i.e., $J>1$, the approach is similar to the case with only one memory variable. For each memory variable $M_n^{(j)}$, we substitute the second equation into the first equation of (1.2) recursively for $n-1$, $n-2$, ..., 2, 1, to obtain the

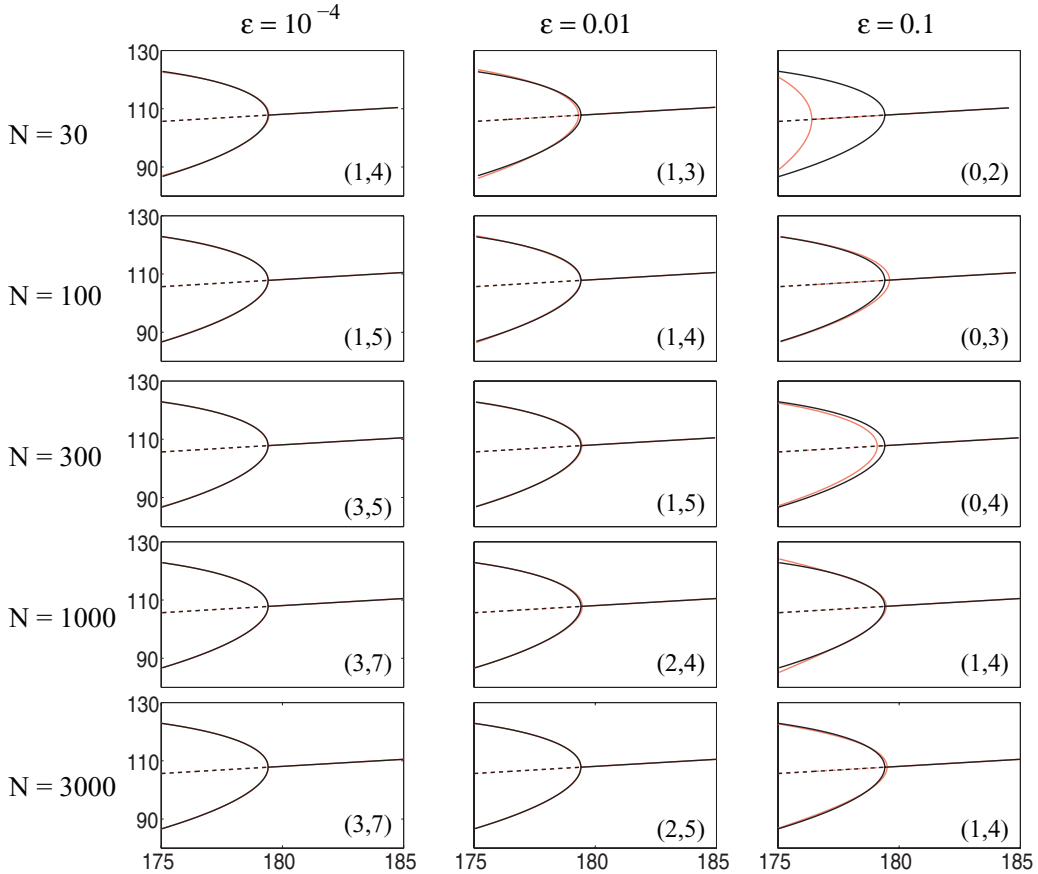

FIG. 10. (Color online) Bifurcation diagrams of the optimal approximate H_k^p (red, light grey) compared to the exact result (black) for various values of ϵ and N. In some of the graphs the approximate and exact diagrams almost coincide. The corresponding optimal choice of (k,p) is shown in the bottom right corner of each graph.

relationship

$$A_n = F_n\big(A_0; M_0^{(1)}, M_0^{(2)}, \ldots, M_0^{(J)}; A_{n-1}, A_{n-2}, \ldots, A_1; T_{n-1}, T_{n-2}, \ldots, T_0\big).$$

Following a similar argument as above, we assume that in the long time run, i.e., when n is sufficiently large, this function can be approximated by a polynomial H_k^p in the same form as (3.5), with k memories and polynomial of degree p. We apply the same methodology as in Sec. III: we determine the unknown coefficients $h_{\alpha\beta_1\beta_2\cdots\beta_k}$ using regression and compute the RSS, RSE, and BIC values for each (k,p). We then obtain the optimal choice of (k,p) by minimizing the BIC value.

V. DISCUSSION

For a general mapping model (1.2), we assume there are iterative maps H_k in (3.4) and we approximate each H_k by the polynomial H_k^p in (3.5) for various orders p. A necessary condition for the existence of H_k's is that the coefficients of H_k^p's obtained by the regression method have the following consistency property: the coefficient for the same term is close in each H_k^p, or it has some tendency of convergence as k and p become larger. For example, we expect that $h_{1,0,\ldots,0}$, the coefficient of $(A_{n-1} - \bar{A})$ in each H_k^p, should not vary much as $k, p \to \infty$. In Fig. 8, we show the values of the coefficients of $(A_{n-1} - \bar{A})$ and $(A_{n-1} - \bar{A})(T_{n-1} - \bar{T})$ versus p for different values of k for the Fox *et al.* model described in Sec. III. Consistency can be observed in each coefficient.

The role of ϵ in (2.9) is important. When ϵ is small, earlier memories are able to be detected and higher order accuracy can be obtained; when ϵ is large, the noise in the measurement may mask the memory so that it cannot be detected. For the model of Fox *et al.* discussed in Sec. III, if $\epsilon = 10^{-4}$, we find that $k = 3$ and $p = 6$ is optimal, while if $\epsilon = 0.1$, we find that $k = 1$ and $p = 4$ is optimal. In Figs. 9(a)–9(d) we show the RSE and BIC values versus p for various k for each case, respectively. We also show bifurcation diagrams at the optimal choice of (k,p) for each case in Figs. 9(e) and 9(f), compared to the theoretical bifurcation diagrams. It is not surprising that a better approximation can be obtained with less noise.

The number of data points, N, is also important. Roughly speaking, if there are more data points for a fixed time interval, we can obtain better accuracy of the approximate dynamics. Table V shows the optimal choice of (k,p) and the corresponding RSE for a variety of N. In Fig. 10 we show the bifurcation diagrams of the optimal approximate H_k^p for various ϵ and N. Clearly, for larger measurement error (ϵ), more data points (N) are needed in order to ensure a good approximate bifurcation curve.

The method we described here does not require any particular distribution for the stochastic pacing cycles T_n, although in Secs. II and III, we used the uniform distribution as an example. We tested some other distributions. In Fig. 11 we show the results for some other distributions of pacing cycles, where we use the Fox *et al.* model with testing time interval $[\mu_a, \mu_b] = [175, 185]$, number of data points $N = 1000$, and $\epsilon = 0.01$. We find that in each case our method gives reliable results, although the best choice of k and p can differ.

Although our method is based on a discussion of small variation in pacing cycles, exciting results are obtained when

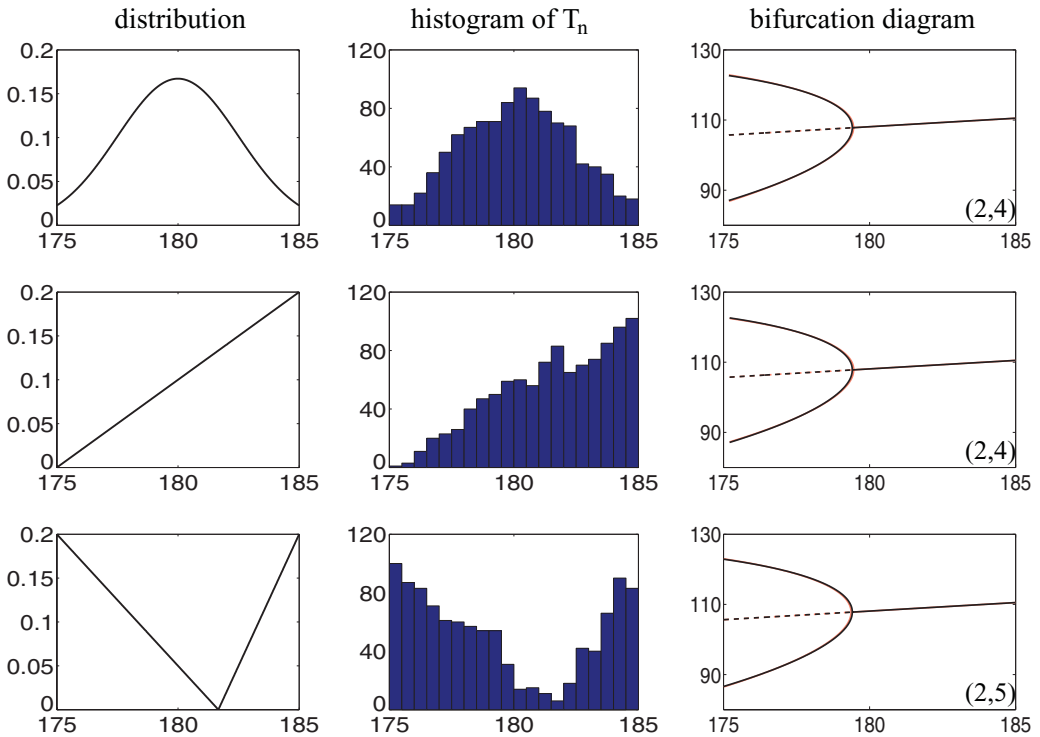

FIG. 11. (Color online) Probability density function and histogram of the applied pacing cycles, and bifurcation diagram of the optimal approximate H_k^p (red, light grey) compared to the exact curve (black) for three different distributions of pacing cycles, where $N = 1000$ and $\epsilon = 0.01$. The optimal choice of (k,p) is labeled in each graph of the bifurcation diagram. We note that the approximate and the exact bifurcation diagrams are very close and hard to distinguish in all the graphs.

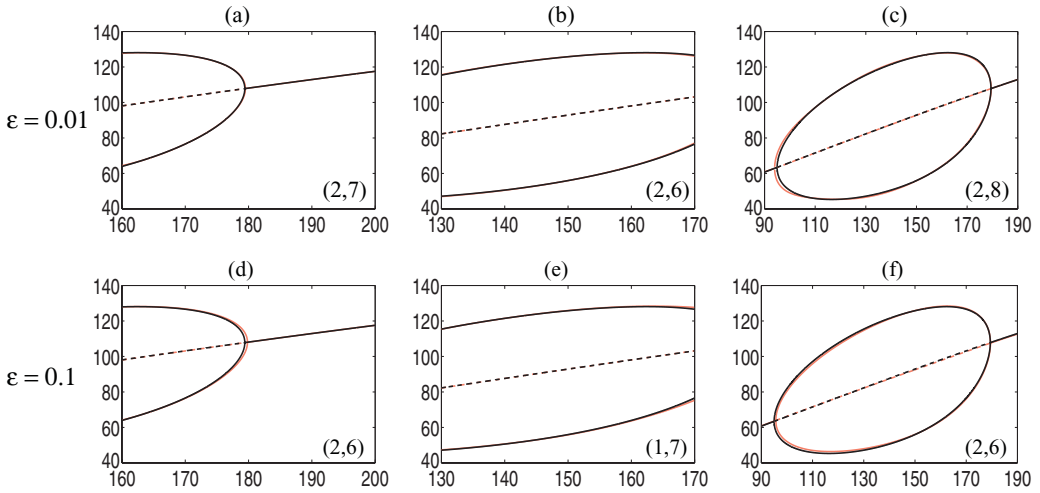

FIG. 12. (Color online) Bifurcation diagrams of the optimal approximate H_k^p (red, light grey) compared to the exact result (black) for various testing time intervals, for $\epsilon = 0.01$ (a, b, c) and 0.1 (d, e, f), respectively, and in all cases $N = 1000$. In some graphs the approximate and exact diagrams almost coincide. The optimal choice of (k, p) is shown in the bottom right corner of each graph.

the method is applied to larger regions of pacing cycles. In Fig. 12 we show the results for different time intervals $[\mu_a, \mu_b] = [160,200],[130,170],[90,190]$ for $\epsilon = 0.01$ and 0.1, respectively, and the approximation matches the theory quite well in each case.

VI. CONCLUSION

In this paper, we provide an approach to investigate APD restitution and bifurcations when there is memory. We use stochastic pacing cycles to simulate the model to obtain the data (a series of APDs) and we find an approximate polynomial using a regression method. We are then able to produce bifurcation diagrams corresponding to the approximate restitution function. We demonstrate the process with data generated by the models of Tolkacheva *et al*. and Fox *et al*. The procedure is summarized as follows: (1) Generate a random series of pacing cycles in a time interval of interest from some distribution. (2) Apply stimuli with this pacing protocol and record the corresponding APDs. (3) Compute $\bar{T}$ and $\bar{A}$, the sample mean of the pacing cycles and APDs, respectively, and then for each (k, p) find a polynomial in the form (3.5) by regression and obtain the RSS and RSE values. (4) Compute the BIC value for each approximation and determine the optimal (k, p) which has minimal BIC value. (5) Use the corresponding polynomial H_k^p to approximate the dynamics and determine the bifurcation structure.

The method of stochastic pacing we introduce here has several advantages over previous protocols: (1) The pacing protocol is simple, as we only need to generate a few hundred pacing cycles; (2) the approximate dynamics is obtained in an entire time interval of interest, not merely at a single point; (3) we are able to deal with cases when the fixed point is unstable and alternans appears, thereby detecting bifurcations; and (4) we have a high order of accuracy.

While we illustrated this method using data from specific models, one could also generate the data using full ionic models, or directly from *in vitro* experiments. We also expect that this method can be used to analyze data from *in vivo* experiments. *In vivo*, the pacing protocol is not externally generated but, because it is variable, the same ideas can be applied. In future work, we will use this method to study several important ionic models.

ACKNOWLEDGMENTS

We would like to thank the referees for their very valuable comments and suggestions. This work is under the support of the National Science Foundation under Agreement No. 0635561, Grants No. NSF-DMS-0931642, No. NSF-DMS-0718036 and No. NSF-DMS-1122297.

APPENDIX

1. Tolkacheva *et al.*'s model

The mapping model of Tolkacheva *et al*. [21] is in the form

$$\widetilde{A}_{n+1} = f(\widetilde{A}_n, \widetilde{D}_n) = C_1 - \frac{r_{\rm cur}}{P(\widetilde{A}_n, \widetilde{D}_n)} + \sqrt{1 - \frac{C_2}{P(\widetilde{A}_n, \widetilde{D}_n)} + \left[\frac{r_{\rm cur}}{P(\widetilde{A}_n, \widetilde{D}_n)}\right]^2}, \quad \text{(A1)}$$

where $\widetilde{A}_n = A_n/\tau_{\rm sclose}$ and $\widetilde{D}_n = D_n/\tau_{\rm sclose}$ are dimensionless variables, and

$$P(\widetilde{A}, \widetilde{D}) = 1 - (1 - G(\widetilde{A})e^{-\widetilde{A}})e^{-Dr_{\rm gate}}, \quad \text{(A2)}$$

$$G(\widetilde{A}) = \frac{r_{\rm cur}\widetilde{A} - (1 - v_{\rm crit})r_{\rm mix}}{1 - \exp[-\widetilde{A} + r_{\rm mix}(v_{\rm sig} - v_{\rm crit})/r_{\rm cur}]}, \quad \text{(A3)}$$

with the constants

$$C_1 = 1 + \frac{r_{\rm mix}}{r_{\rm cur}}(v_{\rm sig} - v_{\rm crit}), \qquad C_2 = 2[r_{\rm cur} + r_{\rm mix}(v_{\rm sig} - 1)]. \quad \text{(A4)}$$

Typical values of the parameters are listed in Table VI.

TABLE VI. Typical parameter values in Tolkacheva *et al.*'s model.

Parameter	Value (ms)	Parameter	Value (dimensionless)
τ_{sclose}	1000	v_{crit}	0.13
τ_{slow}	127	v_{sig}	0.85
τ_{ung}	130	κ	40
τ_{sopen}	50	v_{vout}	0.1
τ_{fopen}	18		
τ_{fclose}	10		
τ_{fast}	0.25		

2. Fox *et al.*'s model

The mapping model by Fox *et al.* [22] is in the following form:

$$\begin{aligned} A_n &= f(D_{n-1}, M_n), \\ M_n &= g(M_{n-1}, D_{n-1}, A_{n-1}), \\ D_n &= T_n - A_n, \end{aligned} \tag{A5}$$

TABLE VII. Typical parameter values in Fox *et al.*'s model.

Parameter	Value	Units
c_0	0.9	dimensionless
c_1	88	ms
c_2	122	ms
c_3	40	ms
c_4	23	ms
τ	160	ms

where

$$f(D,M) = (1 - c_0 M)\left(c_1 + \frac{c_2}{1 + e^{-(D-c_3)/c_4}}\right), \tag{A6}$$

$$g(M,D,A) = e^{-D/\tau}[1 + (M-1)e^{-A/\tau}]. \tag{A7}$$

Typical values for the parameters are given in Table VII.

[1] D. Noble, J. Physiol. **160**, 317 (1962).
[2] G. W. Beeler and H. Reuter, J. Physiol. **268**, 177 (1977).
[3] C. H. Luo and Y. Rudy, Circ. Res. **74**, 1071 (1994).
[4] V. Iyer, R. Mazhari, and R. L. Winslow, Biophys. J. **87**, 1507 (2004).
[5] A. Mahajan, Y. Shiferaw, D. Sato, A. Baher, R. Olcese, L. H. Xie, M. J. Yan, P. S. Chen, J. G. Restrepo, A. Karma, A. Garfinkel, Z. Qu, and J. N. Weiss, Biophys. J. **94**, 392 (2008).
[6] C. H. Luo and Y. Rudy, Circ Res. **74**, 1097 (1994).
[7] J. B. Nolasco and R. W. Dahlen, J. Appl. Physiol. **25**, 191 (1968).
[8] M. R. Guevara, G. Ward, A. Shrier, and L. Glass, IEEE Computers in Cardiology **562**, 167 (1984).
[9] D. R. Chialvo, D. C. Michaels, and J. Jalife, Circ. Res. **66**, 525 (1990).
[10] N. F. Otani and R. F. Gilmour, Jr., J. Theor. Biol. **187**, 409 (1997).
[11] R. F. Gilmour, Jr., N. F. Otani, and M. A. Watanabe, Am J Physiol. **272**, H1826 (1997).
[12] G. M. Hall, S. Bahar, and D. J. Gauthier, Phys. Rev. Lett. **82**, 2995 (1999).
[13] M. A. Watanabe and M. L. Koller, Am. J. Physiol. Heart Circ. Physiol. **282**, H1534 (2002).
[14] E. Cytrynbaum and J. P. Keener, Chaos **12**, 788 (2002).
[15] Y. Shiferaw, Z. Qu, A. Garfinkel, A. Karma, and J. N. Weiss, Ann. N.Y. Acad. Sci. **1080**, 376 (2006).
[16] Z. Qu, Y. Shiferaw, and J. N. Weiss, Phys. Rev. E **75**, 011927 (2007).
[17] T. Kuusela, Phys. Rev. E **69**, 031916 (2004).
[18] C. Lerma, T. Krogh-Madsen, M. Guevara, and L. Glass, J. Stat. Phys. **128**, 347 (2007).
[19] N. Karim, J. A. Hasan, and S. S. Ali, J. Basic Appl. Sci. **7**, 71 (2011).
[20] L. A. N. Amaral, A. L. Goldberg, P. C. Ivanov, and H. E. Stanley, Comput. Phys. Commun. **121**, 126 (1999).
[21] E. G. Tolkacheva, D. G. Schaeffer, D. J. Gauthier, and W. Krassowska, Phys. Rev. E **67**, 031904 (2003).
[22] J. J. Fox, E. Bodenschatz, and R. F. Gilmour, Jr., Phys. Rev. Lett. **89**, 138101 (2002).
[23] D. C. Trost, J. Biopharm. Stat. **18**, 773 (2008).
[24] E. G. Tolkacheva, D. G. Schaeffer, D. J. Gauthier, and C. C. Mitchell, Chaos **12**, 1034 (2002).
[25] D. G. Schaeffer, J. W. Cain, D. J. Gauthier, S. S. Kalb, R. A. Oliver, E. G. Tolkacheva, W.-J. Ying, and W. Krassowska, Bull. Math. Biol. **69**, 459 (2007).
[26] S. S. Kalb, E. G. Tolkacheva, D. G. Schaeffer, D. J. Gauthier, and W. Krassowska, Chaos **15**, 023701 (2005).
[27] S. S. Kalb, H. M. Dobrovolny, E. G. Tolkacheva, S. F. Idriss, W. Krassowska, and D. J. Gauthier, J. Cardiovasc. Electrophysiol. **15**, 698 (2004).
[28] G. E. Schwarz, Ann. Stat. **6**, 461 (1978).